A&A 409, 771–780 (2003)
DOI: 10.1051/0004-6361:20031133

Astronomy & Astrophysics

Measurement of Stark parameters of HeII P_α, P_β and P_γ spectral lines

F. Rodríguez, J. A. Aparicio, V. R. González, J. A. del Val⋆, and S. Mar

Departamento de Optica y Física Aplicada, Facultad de Ciencias, Universidad de Valladolid, 47071 Valladolid, Spain

Received 24 March 2003 / Accepted 7 July 2003

Abstract. This work reports information on the pressure broadened profiles of the HeII P_α, P_β and P_γ spectral lines measured in a pulsed discharge lamp. Information relative to the line shapes, full width at 1/2, 1/4 and 1/8 of the maximum intensity and the dip of the HeII 320.3 nm is provided. The electron density has been determined by two-wavelength interferometry and from the Stark width of the HeI 501.6 nm. and ranges during the HeII emission from 0.54 to 0.64×10^{23} m^{-3} in the plasma. Temperature (1.7–2.4 eV) has been simultaneously determined from the Boltzmann-plot of HeI and from local thermodynamic equilibrium (LTE) assumptions. The final results have been compared with most of the previous existing data.

Key words. atomic data – line: profiles – plasmas – methods: laboratory

1. Introduction

Optical diagnostics is a known and powerful tool to obtain information concerning the processes involved inside and around a plasma. In the case of helium plasmas, they are present in industrial applications, like welding or cutting processes and in scientific research, like the inertial confinement plasmas or astrophysical analysis. In this last field, HeII emission appears very often (Tylenda et al. 1994) in many O-type or Wolf-Rayet stars, galaxies or in the central parts of planetary nebulae, where the effective temperature is typically higher than 2 eV. HeII line parameters are specially useful (Kunasz 1980; Shrader et al. 1997) in these cases to characterize the plasma and to extract information about abundances, radiative processes, etc.

Due to its hydrogen features, much interest has been paid in the past to the Stark parameters of HeII lines, e.g. Stark widths, shifts, dips and functional dependencies of their line wings. In the case of P_α and P_β lines, great effort has been focused on obtaining accurate measurements of these quantities (Berg et al. 1962; Eberhagen & Wunderlich 1970; Bogen 1970; Jones et al. 1971; Einfeld & Sauerbrey 1976; Bacon et al. 1977; Soltwisch & Kusch 1979; Oda & Kiriyama 1980; Bernard et al. 1981; Piel & Slupek 1984; Ackermann et al. 1985; Pittman et al. 1980, 1986; Gawron et al. 1988; Glenzer et al. 1992, 1994; Hammel et al. 1993; Godbert et al. 1994; Konjević et al. 1995; Stefanović et al. 1995; Büscher et al. 1996; Wrubel et al. 1997) in order to validate or not different theoretical proposals (Griem et al. 1962; Kepple 1972; Greene 1976; Schöning & Butler 1989a,b; Seaton 1990; Calisti et al. 1990; Stehlé 1996). In the case of the P_γ line, data are much more scarce. Apart from one theoretical calculation (Schöning & Butler 1989a,b) performed at electron densities lower than 10^{22} m^{-3} and one experimental determination of the Stark broadening parameter performed at temperatures higher than 15 eV (Eberhagen & Wunderlich 1970), there is no further information in the literature concerning this line, up to the authors' knowledge.

This work reports Stark broadening parameters and Stark profiles of the first three spectral lines of the HeII Paschen series as well as the dip measurements of the P_β 320.3 nm. All measurements were performed in a highly reliable pulsed arc, with good reproducibility in successive discharges. Electron density was measured independently from two-wavelength interferometry and from the HeI 501.6 nm Stark broadening, being around 0.6×10^{23} m^{-3}. The excitation temperature was simultaneously measured from the HeI Boltzmann-plot and from the LTE hypothesis and is around 2 eV in this experiment. By comparing these plasma parameters with those reached in previous experimental works, it is easy to notice that temperatures considered here are the lowest ones for which Stark parameters have been measured in the case of HeII Paschen lines. This allows us to extend the range of temperatures where comparisons between experimental measurements and theoretical calculations can be performed, this is interesting by itself, especially in the case of hydrogen lines where Stark broadening theoretical models have been demonstrated to be very good predictors of the electron density in plasma diagnostics.

Special attention has been paid to the experimental aspects like self-absorption effects, intensity and wavelength

Send offprint requests to: Dr. J. A. Aparicio,
e-mail: apa@opt.uva.es

⋆ *Permanent address:* Departamento de Física Aplicada, Universidad de Salamanca, E. Politécnica Superior 05071 Avila, Spain.

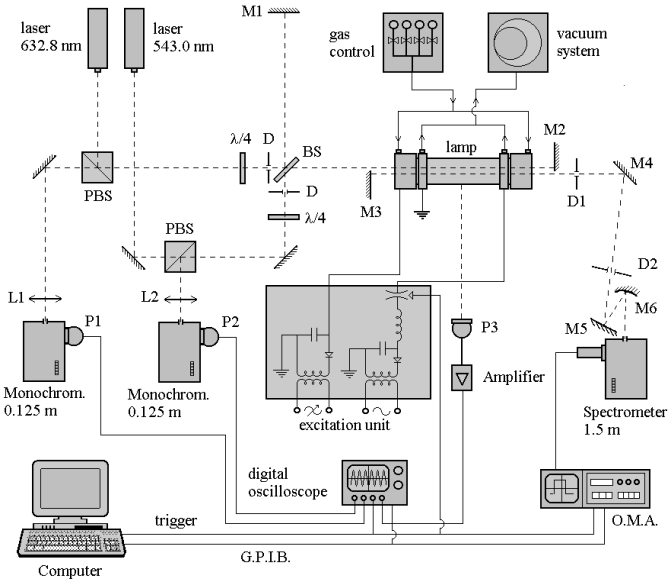

Fig. 1. Experimental set-up.

calibration of the spectrometric system as well as the influence of other broadening mechanisms. Finally, apart from full widths at half, 1/4 and 1/8 of the maximum intensity and the P_β dip which have been determined and compared with most of the previous existing data, experimental profiles have also been supplied and compared with calculations. They may be useful in future theoretical modelling.

2. Description of the experimental set-up and measurements

2.1. Experimental arrangement and calibrations

A scheme of the set-up and diagnostic techniques employed here is shown in Fig. 1. The most important details relative to the experimental apparatus, plasma generation and synchronization of the whole experiment were previously published (Gigosos et al. 1994; del Val et al. 1998). Here we will only give the most interesting details concerning the present experiment.

The plasma pulse was created from the discharge of a capacitor bank of 20 μF charged up to 8000 V. The gas is preionised between consecutive plasma pulses in order to assure good reproducibility of discharges. The lamp was continuously traversed by a flow of pure helium at a rate of 2 cm^3/min and a pressure of 1.16×10^3 Pa. These experimental conditions were selected in order to obtain minimal or negligible self-absorption and maximal intensity in the Paschen HeII lines. In these conditions, HeII lines are emitted in the interval from 20 μs to 65 μs after the discharge is generated.

Spectroscopic and interferometric end-on measurements were made on the lamp at two different plasma columns 3 mm diameter placed 2 mm off the lamp axis in symmetrical positions referred to it. A high cylindrical symmetry of the electron density and temperature has already been proved to exist in this lamp (del Val et al. 1998). In order to determine the refractivity changes due exclusively to free electrons and, from them, the electron density evolution curve $N_e(t)$ during a pulse, interferometric measurements of the plasma were made at two wavelengths (632.8 and 543.0 nm). Spectra were obtained with the help of a Jobin-Yvon monochromator of 1.5 m focal length and a 2400 lines/mm holographic grating, equipped with an optical multichannel analyzer (OMA), and a detector divided into 512 channels (EG&G 1455R-512-HQ). The inverse linear dispersions in its first order of diffraction at λ = 468.6, λ = 320.3 and λ = 273.3 nm are 5.47, 6.20 and 6.37 pm/channel respectively. Mirror M3 in Fig. 1 is employed to detect (Aparicio et al. 1998) self-absorption and to reconstruct (González et al. 1999, 2000) spectral profiles if necessary. The entrance slit was selected 70 μm width in order to obtain spectra with the highest intensity and minimal instrumental function. This was measured by introducing 632.8 nm and 543.0 nm laser radiation in the spectrometer in its first order of diffraction. The instrumental width ω_i was measured to be 3 OMA channels.

This spectrometer was previously calibrated both in wavelength and in intensity by the procedures described by Aparicio et al. (1997, 1998). In the case of the intensity calibration, the light emitted by incandescent and deuterium lamps from which an absolute previous calibration is available was registered. Inverse linear dispersions and relative spectral transmittances are known with uncertainties around 1% and 4% respectively.

2.2. Measurements performed

Each HeII line was recorded in 3 different instants along the plasma life (25, 40 and 60 μs after the beginning of the discharge) and, for each instant, in 60 different runs, 30 with mirror M3 and 30 without it, in order to obtain profiles with the best signal-to-noise ratio. Several HeI lines (388.8, 471.3, 501.6, 667.8, 706.5 and 728.1 nm) were also recorded at the same instants in 10 different runs, 5 with and 5 without mirror M3. The HeII lines were measured to determine the Stark parameters. The HeI ones have been used to determine HeI excitation temperature T_{exc}^{HeI} and the electron density from the 501.6 nm Stark width. In all cases, spectra were taken in the first order of diffraction of the spectrometer. Time exposures were always 5 μs long in order to get good enough temporal resolution. For every HeII spectrum registered, two interferograms 500 μs long were also taken, each one corresponding to the two wavelengths operated in the interferometer.

3. Data processing and plasma diagnostics

3.1. Pre-processing

As a common pre-processing for all the lines measured, self-absorption was checked in all cases. For each line and each instant, the average of spectra taken with and without mirror M3 were calculated. Individual spectra differed from their average less than 5% for the P_α and less than 7% for the P_β and P_γ in all cases. By comparing the spectra taken with and without the self-absorption mirror, optical depths were measured. Minimal self-absorption was detected for P_α spectra, changing their reconstructed profiles at the peak intensity less than 5% from the original ones.

Table 1. Excitation temperatures T_{exc}^{HeI}, equilibrium temperature T^{LTE} and electron densities for the three different instants of the plasma life where HeII spectra were taken. Uncertainties for temperatures and electron densities have been estimated around 15% and 10% respectively.

Time (μs)	T_{exc}^{HeI} (eV)	T^{LTE} (eV)	N_e ($\times 10^{23}$ m^{-3})
25	1.85	1.72	0.54
40	2.43	1.95	0.64
60	1.71	1.73	0.55

Afterwards, the average of spectra taken without mirror M3 were divided by the transmittance function in order to put all spectra in a scale which allows us to determine their relative intensities and to perform temperature calculations. All HeI lines were then fitted (Gigosos et al. 1994) to sums of Lorentzian functions plus a linear luminous background which takes into account recombination and bremstrahlung effects. This is justified since the Stark effect is the dominant broadening mechanism at the electron densities and temperatures reached in this plasma. Differences between the experimental spectra and the fits were usually lower than 1%. The fitting algorithm allows us to determine simultaneously the center, asymmetry, experimental line width ω_{exp} and area under each profile.

3.2. Temperature

In relation to Stark parameters of spectral lines, the most significant temperature is the kinetic electron temperature. In collision dominated plasmas like the one generated by this plasma source, it is usually assumed that the excitation temperature is a good approach to the kinetic electron temperature (van der Mullen 1990). Excitation temperature has been calculated from the Boltzmann-plot of HeI lines at each instant where HeII profiles were registered. Very good linear behaviors were found in the fits, which suggests that the hypothesis of partial local thermodynamic equilibrium (pLTE) assumed when performing these Boltzmann-plots is verified. This situation has already been confirmed in previous experiments performed in this laboratory (Gigosos et al. 1994; Aparicio et al. 1997; del Val et al. 2000, 2001; Mar et al. 2000; Rodríguez et al. 2001). Temperature T^{LTE} has been additionally calculated by assuming local thermodynamic equilibrium in the plasma. In Table 1, both temperatures are shown. As it can be seen, there exists good agreement between them, which seems to confirm that the excitation temperature may be a good indicator of the electron temperature in this experiment. Uncertainties in temperature determination have been estimated around 15%

As far as kinetic emitter temperature is concerned, this may have a double influence on the Stark broadening measurements. Doppler broadening must be estimated since it contributes to the total linewidth specially for light atoms like helium. Furthermore, hydrogen lines as those measured in this experiment are specially sensitive to ion dynamic effects on the Stark broadening which must be considered specifically in the line centers. This temperature has not been measured in this work and has initially been assumed to be equal to the electron temperature.

3.3. Electron density

As it was explained is Sect. 2, electron density was obtained simultaneously from the HeI 501.6 nm Stark width and from two-wavelength interferometry.

The HeI 501.6 nm Stark width ω_S was obtained from its experimental width ω_{exp} and by considering the instrumental ω_i and Doppler broadening ω_D. The latter was calculated from the HeI excitation temperature by assuming the kinetic emitter temperature was the same as the electron temperature. Concerning HeII profiles, Doppler width is less than 5% of the experimental linewidth for all spectra. It is important to notice that if a two temperature plasma had been considered with kinetic emitter temperature around one half of the electron temperature, the Doppler contribution would have always been less than 4% of ω_{exp}. Therefore, although the kinetic emitter temperature is not really known, Doppler broadening is always negligible in relation to Stark broadening for these plasma conditions and the ambiguity in this temperature is not relevant here. However, since HeI profiles are narrower than HeII ones, these broadening mechanisms have really been taken into account. In fact, HeI Stark widths have been obtained (Davies et al. 1963) by considering the Gaussian width component ω_G of the profile to be given by the known expression $\omega_G = (\omega_D{}^2 + \omega_i{}^2)^{1/2}$. The electron density has been obtained from the Stark width by using results from previous calibrations (Pérez et al. 1991).

In relation to the interferometric registers, they were processed according to the algorithms developed by de la Rosa et al. (1990) and described by Aparicio et al. (1998). They allow us to determine for each wavelength an average curve of the phase evolution changes along the plasma life $\Delta\psi_{\lambda_i}(t)$ ($i = 1, 2$) and from them, the electron density curve $N_e(t)$, according to the expression:

$$n_e(t) = \frac{4\pi\varepsilon_0 m_e c^2}{q_e^2}\frac{1}{2L}\frac{\lambda_2\Delta\psi_{\lambda_1}(t) - \lambda_1\Delta\psi_{\lambda_2}(t)}{\lambda_1^2 - \lambda_2^2}. \quad (1)$$

L, the plasma column length, which as has usually been demonstrated for this plasma source, is assumed to be equal to the lamp length.

In Fig. 2 both experimental determinations of the electron density are shown. As it can be seen in this figure, there exists very good agreement between these independent measurements, which seems to confirm the hypothesis concerning to the plasma column length, as well as the negligible influence of possible boundary layers. This good agreement allows us to estimate the uncertainty in the electron density determination lower than 10%. The electron density obtained from interferometric measurements will be employed for further calculations. The values obtained for the three instants where spectroscopic measurements were made are included in Table 1.

2[htbp]

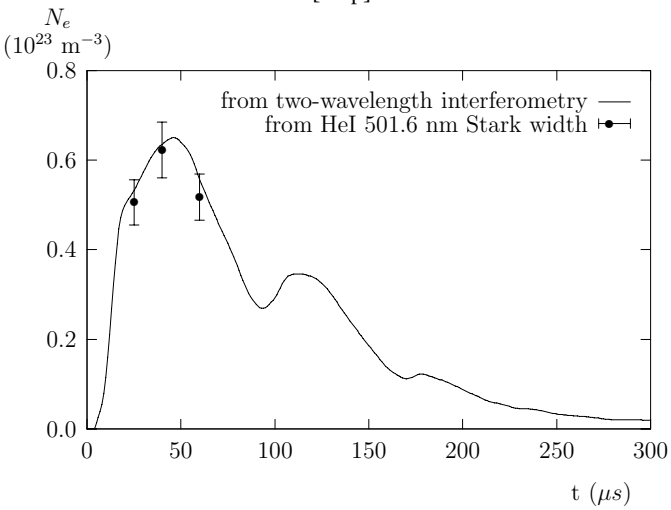

Fig. 2. Electron density evolution curve. Error bars of 10% have been considered for comparison.

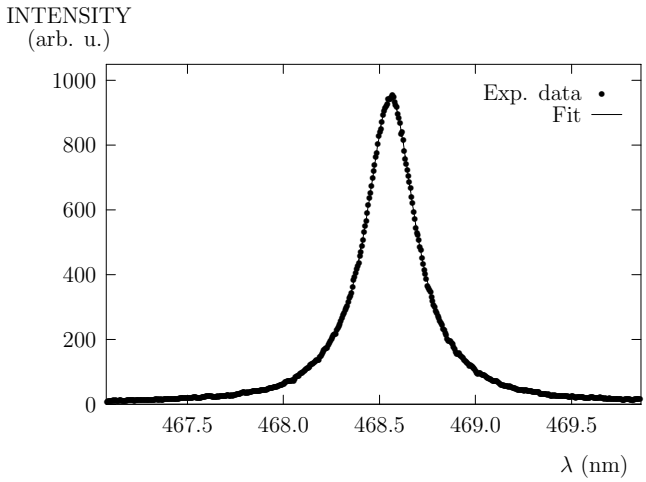

Fig. 3. Experimental spectrum of the HeII 468.6 nm line and its Lorentzian fit.

4. P-lines processing

4.1. P_α processing

In Fig. 3 a spectrum of the HeII 468.6 nm is shown, as well as its fit to the sum of a Lorentzian function plus a linear luminous background. As it can be seen, the agreement between the experimental data and the fit is extremely good simultaneously in the center and in the wings. Electron broadening appears as the dominant broadening mechanism in these plasma conditions. Stark parameters were obtained in the same way as explained for the HeI 501.6 nm. Additionally, full widths at 1/4 and 1/8 of the maximum intensity were also determined.

4.2. P_β processing

In the upper part of Fig. 4, an experimental spectrum $E(\lambda)$ of the HeII 320.3 nm is shown. As it can be seen, the HeI line 318.8 nm appears in the blue wing. However, no molecular helium lines are observed, as was pointed out by Stefanović (1995).

In order to process these spectra and to obtain isolated profiles of the P_β line, the following procedure was employed. As a first step, and by using an initial estimation $\omega_{\rm ini}$ of the halfwidth and the line center $c_{\rm ini}$ in OMA channels units, these units were transformed to halfwith units c' according to the following expression:

$$c' = \frac{(c - c_{\rm ini})}{w_{\rm ini}/2}. \quad (2)$$

Afterwards, a plot of the intensity of the red wing of the P_β line was performed as a function of these c' units as well as a potential fit, resulting in an exponent of the potential function of –1.91 with a fit correlation factor around 99.6%, which confirmed the Lorentzian decay of the P_β line wings. Since all HeI lines processed to obtain $T_{\rm exc}^{\rm HeI}$ were successfully fitted to Lorentzian functions, the HeI 318.8 nm was also assumed to take this functional behavior. For the dip detected in the P_β line center, a negative Gaussian function was assumed to reproduce it. Since this kind of function decays much more quickly than Lorentzian ones, this assumption for the dip would not perturb in principle the P_β line wings decay. All these previous results allowed us to adjust the experimental spectra $E(\lambda)$ of the HeII 320.3 nm line to mathematical functions $F(\lambda)$:

$$F(\lambda) = L_1(\lambda) + L_2(\lambda) + G(\lambda) + B(\lambda) \quad (3)$$

$L_1(\lambda)$ being the Lorentzian function representing the HeI line, $L_2(\lambda)$ and $G(\lambda)$ the Lorentzian and negative Gaussian components representing the HeII line and $B(\lambda)$ a linear function representing the luminous background. As it can be seen in the figure, the resulting Gaussian component decayed much quicker than the corresponding Lorentzian function $L_2(\lambda)$ confirming the hypothesis performed previously. In the middle of the Fig. 4, the residuals $R(\lambda)$ obtained in percentage as:

$$R(\lambda) = \frac{(E(\lambda) - F(\lambda)) * 100}{F(\lambda)} \quad (4)$$

are shown as a function of wavelength. They appear as a randomized distribution of values around zero in the whole spectrum and below 10%, except perhaps in the far wings where relative uncertainty in the line intensity measurement is greater. In the lower part of this figure, the original spectrum, the fit and the difference $D(\lambda) = E(\lambda) - L_1(\lambda) - B(\lambda)$, are depicted. The quality of the fit is evident. $F(\lambda)$ can scarcely be distinguished under the original profile. From the resulting spectra $D(\lambda)$, the area, $FWHM$ and the widths at 1/4 and 1/8 of maximum intensity were obtained from conventional algorithms.

4.3. P_γ processing

In Fig. 5, a spectral profile of the P_γ line is shown. It is important to remark that no HeI or other lines were detected in the neighborhood of this line at any instant of the plasma emission, so these profiles can be considered completely isolated.

As a first step, the profiles were tried to be fitted to Lorentzian functions, but these fits yielded great discrepancies

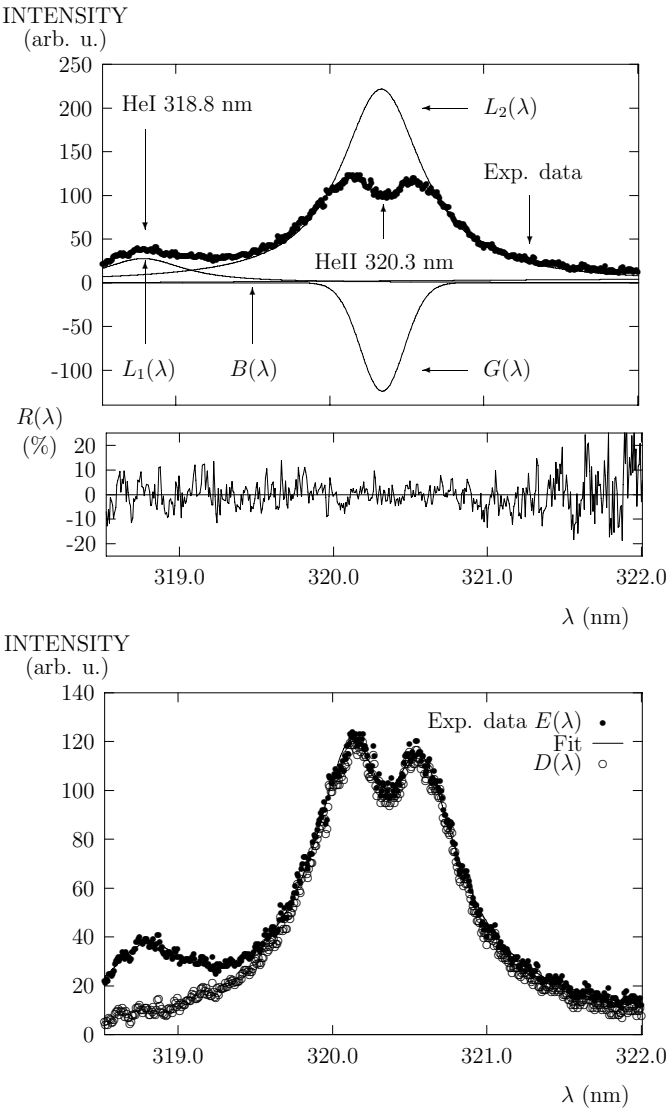

Fig. 4. In the upper part of the figure, the experimental spectrum is shown as well as the functions forming the fit $F(\lambda)$. In the middle, the percentage of residuals is shown. In the lower part, the original spectrum is shown with the fit and the difference $D(\lambda)$.

with experimental measurements. However, and following the previous experience with the other two Paschen profiles measured in this work, the background was calculated by assuming a Lorentzian behavior in the HeII 273.3 nm line wings. Once this background was subtracted from the original profile, area, *FWHM* and widths at 1/4 and 1/8 of the maximum intensity were also calculated.

5. Results and conclusions

In order to make comparisons with previous theoretical and experimental data or calculations, we will try to show our data in the scales and units usually employed in the literature. For instance, for the Stark *FWHM* values, comparisons will be made in nanometers, those corresponding to Stark profiles will be

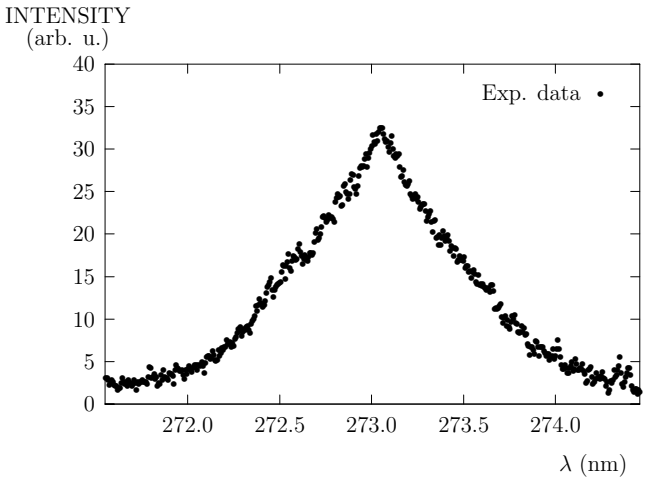

Fig. 5. Experimental spectrum of the HeII 273.3 nm line.

Table 2. Experimental Stark *FWHM* values for the three Paschen lines measured and the three instants considered. The P_β dips have also been included. Uncertainties around 15% have been assigned to these results.

Time (μs)	ω_{P_α} (nm)	ω_{P_β} (nm)	ω_{P_γ} (nm)	dip(%)
25	0.30	0.92	0.90	12.5
40	0.33	0.99	1.00	15.7
60	0.30	0.91	0.82	16.3

made in α units (Å/cgs field), according to the known expressions:

$$\alpha = \Delta\lambda / F_0 \tag{5}$$

$$I_0 = \int I_\lambda \mathrm{d}\lambda \tag{6}$$

$$S(\alpha) = I_\lambda F_0 / I_0 \tag{7}$$

$$F_0 = 2.61 e N_e^{2/3} \tag{8}$$

λ being in Å, N_e in cm^{-3} and F_0 in cgs units. Expression (8) is valid when ionic perturbers correspond to single ionized helium. This is the case in our plasma conditions. Simple calculations from equilibrium equations show that the relation between double and single ionized helium is lower than 0.1%. In this situation F_0 takes a value of 201 cgs field strength units for a electron density of 0.64×10^{23} m^{-3}.

The experimental Paschen Stark *FWHM* values obtained in this experiment as well as the P_β dips are shown in the different columns of Table 2 for the three instants of the plasma emission where measurements were performed. Uncertainties have been estimated around 15%.

5.1. P_α results

As far as *FWHM* values is concerned, comparisons between this work results for P_α line and similar data compiled from the

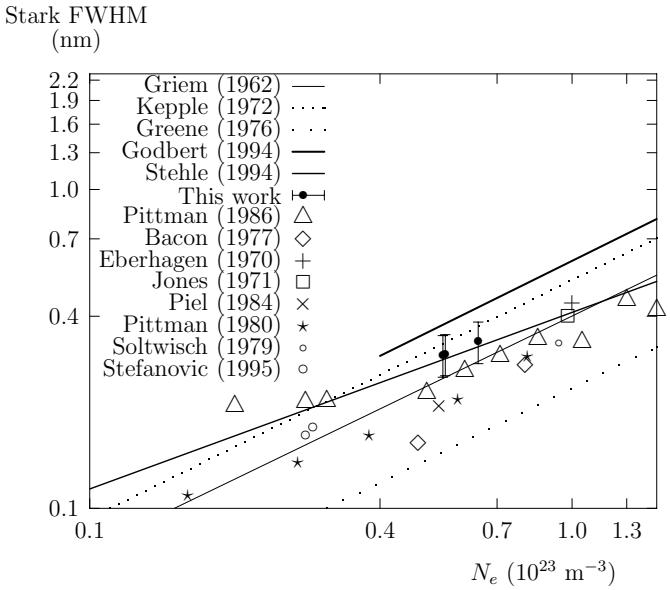

Fig. 6. Logarithmic plot of experimental Stark *FWHM* values and theoretical calculations for the P_α line versus the electron density.

literature have been summarized in Fig. 6. A logarithmic plot has been made containing most of the previous measurements performed in the range of electron densities from 10^{22} to 1.5×10^{23} m^{-3}. Error bars around 15% have been depicted for our data.

If we restrict comparisons only to experimental values obtained at similar electron densities, the best agreement is found with those by Pittman & Fleurier (1986) the differences between their data and ours being around 15%. The influence of self-absorption found by these authors should be probably considered only for electron densities lower than 0.4×10^{23} m^{-3}. Agreement is not so good with Piel (1984) or Pittman et al. (1980), the differences with Bacon (1977) being around 50%. The latter calculated the electron density from the HeI 388.9 nm Stark halfwidth. In spite of the lower accuracy recognized for this method compared with the interferometric determination, this should not justify such a great discrepancy. In all cases our results are greater than others which may partly be explained by the lower temperatures reached in this work. All the experiments cited above were performed at temperatures around 4 eV.

Figure 6 also contains several theoretical approximations. Calculations by Griem et al. (1962), Kepple (1972) and Greene (1976) were performed at 3.4 eV, those by Godbert et al. (1994) were made at 8 eV while Stehlé (1994) did theirs at 8.6 eV. Although these theories are conceptually different, some of them certainly provide very similar results. In fact, our measurements agree surprisingly well with Stehlé's predictions and differ no more than 15% with calculations by Griem et al. (1962) and by Kepple (1972). These three theoretical models differ essentially in the ionic perturber treatment. The first one considers the influence of dynamical ions on Stark broadening, while the last two ones apply the quasi-static approximation, the latter including inelastic electron collision, the interference term between upper and lower levels and the screening of the electric field. Calculations by Greene (1976), based on the unified classical-path theory extended to ionic emitters, and by Godbert et al. (1994), based on the frequency fluctuations and the concept of radiating channels (Calisti et al. 1990) have not succeeded at least in this range of electron densities.

In spite of the scarce numerical data available, we have tried to extend comparisons with theoretical calculations beyond the simple *FWHM* values. They may provide a deeper insight into the physical features involved in our experiment and help theoreticians to improve and refine hypotheses. In order to do this we have proceded as follows. Table 3 contains the experimental full fractional Stark widths at 1/2, 1/4 and 1/8 of the maximum intensity for the three Paschen lines. All data correspond to registers taken 40 μs after the discharge begins ($N_e = 0.64 \times 10^{23}$ m^{-3}, $kT = 2.4$ eV). These conditions were selected because they provided the best signal-to-noise spectra. Theoretical data by Griem et al. (1962) and by Kepple (1972) at 1.7 and 3.4 eV and at 0.64×10^{23} m^{-3} have been included after interpolating their original results between 10^{22} and 10^{23} m^{-3}.

Several conclusions arise from the analysis of results in Table 3. Firstly, it is important to remark that for both theoretical models, predicted fractional widths depend very slightly on temperature, that is to say, P_α profiles remain very insensitive to temperature changes in the range from 1.7 to 3.4 eV. In fact, variations with temperature in calculations by Griem et al. (1962) or by Kepple (1972) are in all cases lower than 8%. Second, differences between Kepple's theoretical data and our experimental results increase continuously from 3% in α_2-values to 20% in α_8-values and the measured fractional widths being usually lower than predicted ones. Finally, comparisons with Griem's predictions only yield good agreement for α_4-values, being broader for the wings and narrower for the central part of the profile.

In Fig. 7 the experimental and several theoretical reduced $S(\alpha)$ Stark profiles are shown. It contains calculations performed by Kepple (1972), by Griem et al. (1962) at $N_e = 0.64 \times 10^{23}$ m^{-3} and at 3.4 eV after interpolation from their original data, and by Greene (1976) also performed at 3.4 eV but at $N_e = 10^{23}$ m^{-3}. None of these theories include the ion dynamical influence on the Stark line broadening, therefore the line centers should show the greatest differences with the experimental register. As it can be seen in this figure, Griem's profiles appear clearly narrower than ours at half maximum. Calculations performed from the unified classical-path theory predict well the wing profile for the data available, but fail seriously in the peak. In spite of a slower decay in the predicted line wings, the best agreement is found with Kepple's line shapes, specially in the line center.

All these results point out that experimental P_α *FWHM* values can be employed as predictors of the plasma electron density in combination with Kepple's theoretical calculations for these electron densities and temperatures, but point also out that there remain some physical aspects in theory or experiments not completely understood.

Table 3. Comparison between experimental full fractional (1/*n*) Stark widths α_n (10^{-2} Å/cgs field strength units) values measured in this work at kT = 2.4 eV for the P_α, P_β and P_γ lines at 0.64×10^{23} m^{-3} with those calculated by Griem et al. (1962) and by Kepple (1972). Theoretical data have been taken from literature by interpolation at this electron density.

Ref.	λ = 468.6			λ = 320.3			λ = 273.3		
	α_2	α_4	α_8	α_2	α_4	α_8	α_2	α_4	α_8
This work	1.66	2.94	4.54	4.91	7.34	10.55	4.95	7.91	10.82
Kepple (1.7 eV)	1.72	3.55	5.67	5.47	8.38	11.68			
Kepple (3.4 eV)	1.64	3.49	5.62	5.57	8.45	11.66			
Griem (1.7 eV)	1.41	3.00	5.13	4.35	7.10	10.30			
Griem (3.4 eV)	1.28	2.92	5.20	4.62	7.35	10.48			

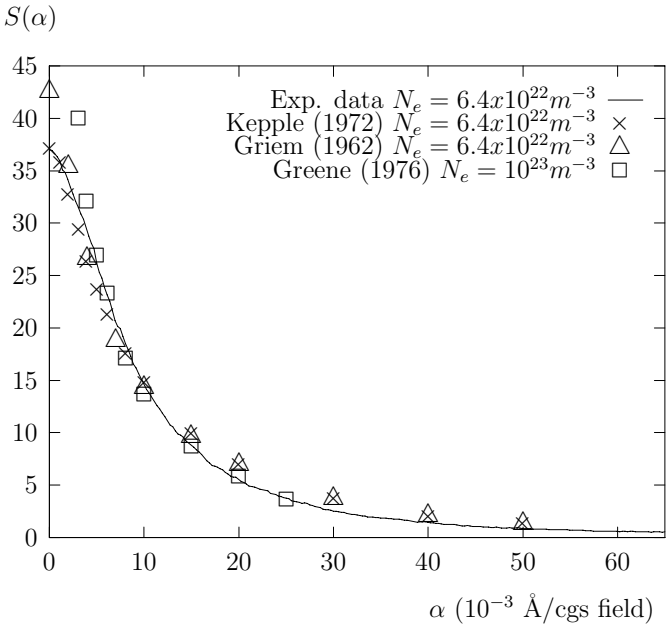

Fig. 7. Comparisons between measured and calculated reduced Stark P_α profiles.

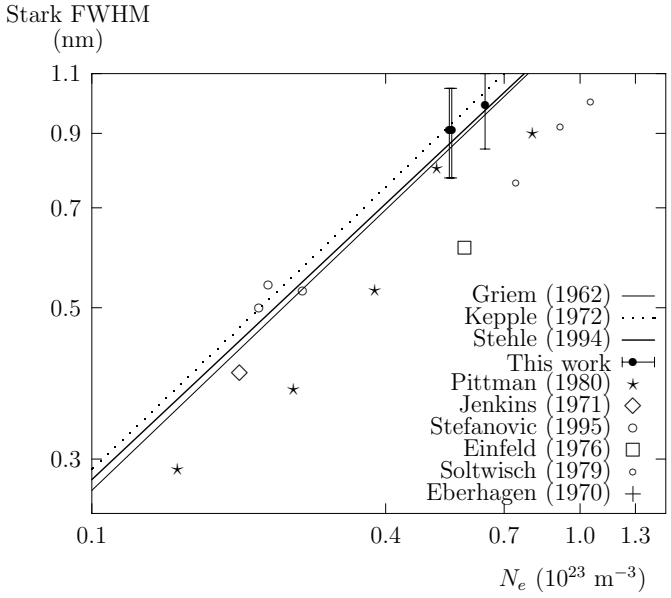

Fig. 8. Logarithmic plot of experimental Stark *FWHM* values and theoretical calculations for the P_β line versus the electron density.

5.2. P_β results

Results concerning the *FWHM* and dip values for the P_β line are respectively listed in the third and fifth columns of Table 2; the comparisons with other experimental or theoretical data are depicted in Fig. 8.

In this case there are not so many data points to compare with at least in the interval of electron densities considered, from 10^{22} to 1.5×10^{23} m^{-3}. In relation to other experimental measurements, very good agreement is found now with one datum from Pittman et al. (1980) showing this result differences lower than 10% with ours, possibly the most optimistic estimation of uncertainty in this kind of measurement and experiment. Once more, comparisons with theoretical calculations reveal very good agreement between our data and those by Kepple (1972) and by Stehlé (1994) although differences with those by Griem et al. (1962) are also lower than the 15% of the uncertainty estimated for our results. A simple look at Fig. 8 allows us to notice that our results joined to those by Stefanović et al. (1995) and by Jenkins (1971) confirm very well the theoretical predictions, while the rest of experimental data including most of Pittman's seem to show in the log-log scale a linear trend very similar to the theoretical one but slightly and systematically below it.

In Table 3 full fractional Stark widths at $N_e = 0.64 \times 10^{23}$ m^{-3} and 2.4 eV have been compared with theoretical estimations by Griem et al. (1962) and by Kepple (1972) at 1.7 and 3.4 eV, obtained by interpolation from their original data. As it can be seen by comparison between the different theories and these experimental results, the influence of temperature in predicted Stark broadened profiles is not significant at least in the interval from 1.7 to 3.4 eV, in a similar way as in the case of the P_α line. At a first glance, our measured fractional Stark widths agree better with Griem's predictions, our results being around 10% lower than Kepple's ones.

In Fig. 9 different theoretical P_β reduced profiles have been plotted in α units as well as one of our measured spectra. Calculations performed by Stehlé (1994) at $N_e = 0.3 \times 10^{23}$ m^{-3} by using the quasi-static and dynamic approaches and by Kepple (1972) and by Griem et al. (1962) at $N_e = 0.64 \times 10^{23}$ m^{-3} obtained by interpolation from their original data have been considered. In all cases calculations were performed at kT = 3.4 eV. The best agreement in the line wing

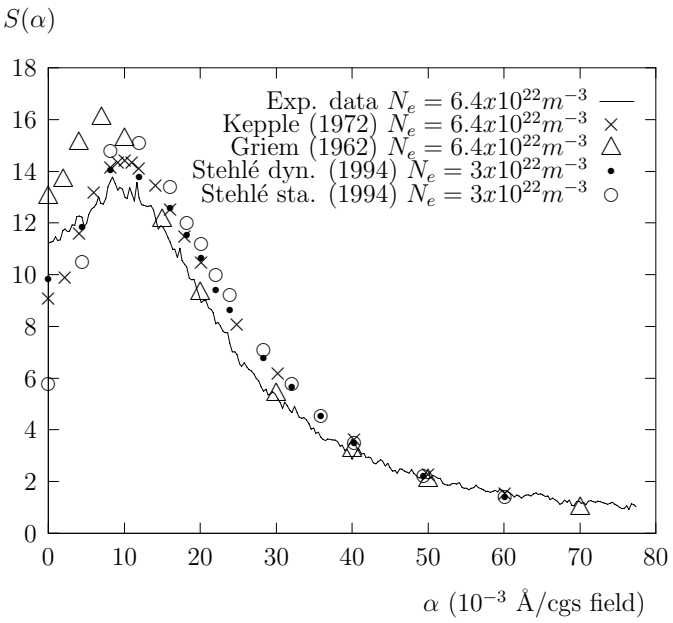

Fig. 9. Comparisons between measured and calculated reduced Stark P_β profiles.

is found now with Griem's calculations the discrepancies being greater in the central structure of the line shape. Agreement with Kepple's profile is poorer along the wing and slightly better than Griem's around the peak. In both cases discrepancies are greater just at the central dip. In relation to Stehlé's profiles, the available data correspond to an electron density slightly lower than that found in our experiment. However their predicted line shapes look broader than ours the central structure being more similar to ours in the case of calculations considering ion dynamics and much more different for the quasi-static approach.

Apart from certain experimental uncertainty linked to the intensity measurement of the line profile and the reproducibility of spectra in different discharges (around 7% for this line), there are other experimental reasons which have usually been argued as possible explanations for a reduced dip structure as that observed in our results, e.g. the influence of the instrumental or the Doppler broadening on the line profile or the plasma inhomogeneities. However, and as it was pointed out in Sect. 3.3, the Gaussian component for all P_β spectra registered in this work is lower than 3% of the experimental linewidths. Concerning possible plasma inhomogeneities along the plasma column, they have never been observed before in this plasma source. Some authors (Stefanović 1995) working with linear discharges have pointed out the existence of molecular helium lines near the HeII 320.3 nm line center in certain experimental conditions as an indicator of cold boundary layers. However they have not been detected in this experiment.

Anyway, it may be of interest to compare the P_β dips measured in this work with previous experimental or theoretical results. These comparisons are shown in Table 4 as ratios of the data listed in Table 2 to different predictions. Calculated values coming from Griem et al. (1962) and from Kepple (1972) have been obtained at the three electron densities considered in this experiment by interpolating their original data. The ones coming from Stehlé (1994) have been taken from her figures always at $N_e = 0.3 \times 10^{23}$ m^{-3}. All of them correspond to predictions performed at $kT = 3.4$ eV. Comparisons with predictions calculated by an experimental scaling proposed by Büscher et al. (1996) after compiling most of the previous experimental results have also been included. This scaling includes the influence of electron density and temperature on the P_β dip.

Apart from ratios lower than unity, like in most of previous experiments, the analysis of data in Table 4 reveals a fairly good agreement between the dips measured in this work and those predicted by the empirical scaling proposed by Büscher et al. (1996). Discrepancies are around or lower than the 15% of uncertainty assigned to the dip measurements. This result suggests that these experimental plasma source offer dips as reliable as other experimental plasma sources do, with similar quality in relation to plasma homogeneity, registered profiles or reproducibility. However, except for predictions performed by the semiclassical theory by Griem et al. (1962), the rest of theoretical calculations predict values for the P_β dips which differ dramatically from our data and from the empirical scaling calculations, even those performed by Stehlé (1994) including ion dynamic effects.

5.3. P_γ results

There is not much information in the literature concerning this spectral line. In fact, the only calculations available in the literature correspond to an application of the unified classical-path theory performed by Schöning & Butler (1989a,b). Unfortunately they only calculated the whole profile for electron densities below 10^{22} m^{-3} so comparisons with this work are not possible. There is only one semiempirical approach which might be used to compare. It corresponds to the experimental work performed in a thetapinch by Eberhagen & Wunderlich (1970) where P_γ profiles were registered in an interval of electron densities from 0.85 to 1.60×10^{23} m^{-3} and a temperature interval from 15 to 23 eV, ten times higher than ours. This empirical scaling relates its Stark $FWHM$ with electron density according to the following expression:

$$N_e(\mathrm{cm}^{-3}) = 1.90 \times 10^{15} (\Delta\lambda_{1/2})^{3/2} \quad (9)$$

$\Delta\lambda_{1/2}$ (in Å) being the $FWHM$ of the HeII 273.3 nm spectral line. This formula which is valid according to the authors for temperatures around 20 eV and electron densities around 10^{23} m^{-3} predicts for our experimental conditions P_γ full halfwidths of 0.93, 1.04 and 0.94 nm respectively for the instants 25, 40 and 60 respectively after the beginning of the discharge. By taking into account the 15% uncertainty considered by these authors for their data and a similar error for our data, the results given in Table 2 fit very well this semiempirical formula.

Since this experiment seems to be the first where measurements of the HeII P_γ profile were performed with a multichannel detector, it may be interesting to include one of them in this work in order to supply specific data for future comparisons of other experiments or calculations. Apart from Fig. 5 which contains one of these registers, the reduced profile $S(\alpha)$

Table 4. Ratios of the three experimental P_β dips measured in this work with other experimental and theoretical calculations. Data from Stehlé (1994) (S) have been taken from the original figures at $N_e = 0.3 \times 10^{23}$ m^{-3}. Those from Griem et al. (1962) (G) and from Kepple (1972) (K) have been obtained by interpolating their original data at the measured electron densities. Predictions by the empirical scaling proposed by Büscher et al. (1996) (B) have also been included.

Time (μs)	$dip_{\rm exp}/dip^{\rm sta}_{\rm (S)}$	$dip_{\rm exp}/dip^{\rm dyn}_{\rm (S)}$	$dip_{\rm exp}/dip_{\rm (G)}$	$dip_{\rm exp}/dip_{\rm (K)}$	$dip_{\rm exp}/dip_{\rm (B)}$
25	0.20	0.49	0.66	0.36	0.81
40	0.26	0.50	0.82	0.42	1.00
60	0.27	0.54	0.74	0.43	0.92

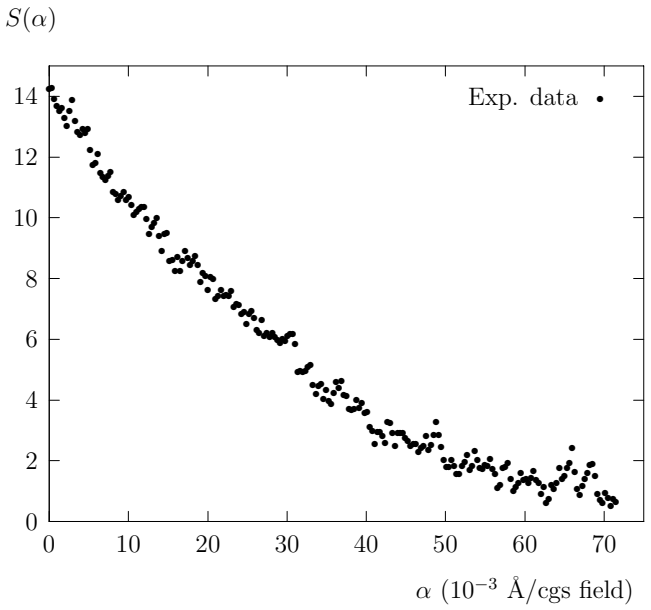

Fig. 10. Reduced profile of the P_γ line for $N_e = 0.64 \times 10^{23}$ m^{-3} and $kT = 2.4$ eV.

of the P_γ red wing is shown in Fig. 10 after substracting the luminous background. It corresponds to an electron density of 0.64×10^{23} m^{-3} and a temperature of 2.4 eV.

6. Conclusions

This work reports information about the Stark profiles of the first three lines of the HeII Paschen series, all of them measured at a temperature lower than that reached in previous experiments. Full widths at half maximum in nanometers, full fractional Stark widths α_2, α_4 and α_8 and the whole reduced profiles $S(\alpha)$ have been provided for these lines and compared with existing experimental or theoretical data when available. An uncertainty of 15% has been estimated for all these parameters and for the P_β dips.

Results and comparisons concerning P_α and P_β lines have concluded that the calculations by Kepple (1972) are able to predict electron densities from their $FWHM$ with uncertainties around 10% at least for the electron densities and temperatures considered in this experiment. However, comparisons between experimental profiles and theoretical calculations have not succeeded. Concerning the P_β dips the best agreement was found with Griem's calculations and with predictions obtained from empirical scalings like that proposed by Büscher et al. (1996), which may suggest that the quality of this plasma source in relation to reproducibility, axial homogeneity and intensity measurements is similar to others previously used for these measurements. However, discrepancies between different theories and experimental results as a whole and between theories themselves remain, more studies being necessary in order to get a better understanding of the physical phenomena involved in Stark broadening processes.

Acknowledgements. The authors thank S. González for his collaboration in the experimental arrangement, and the Spanish Dirección General de Investigación Científica y Técnica (Ministerio de Educación y Ciencia) and the Consejería de Educación y Cultura de Castilla y León for their financial support under contracts No. BFM2002-01002 and VA130-02 respectively. Dr. J. A. Aparicio wants to express his personal acknowledgement to the Organización Nacional de Ciegos de España (ONCE) for help.

References

Aparicio, J. A., Gigosos, M. A., & Mar, S. 1997, J. Phys. B, 30, 3141
Aparicio, J. A., Gigosos, M. A., González, V. R., et al. 1998, J. Phys. B, 31, 1029
Ackermann, U., Finken, K. H., & Musielok, J. 1985, Phys. Rev. A, 31, 2597
Bacon, M. E., Barnard, A. J., & Curzon, F. L. 1977, J. Quant. Spectrosc. Radiat. Transfer 18, 399
Berg, H. F., Ali W., Lincke R. & Griem, H. R. 1962, Phys. Rev. 125, 199
Bernard, J. E., Curzon, F. L., & Barnard, A. J. 1981, in Proc. 5th Int. Conf. on Spectral Line Shapes (Berlin, 1980), ed. Walter de Gruyter & Co. (New York), 152
Bogen, P. 1970, Z. Naturforsch. 25a, 1151
Büscher, S., Glenzer, S., Wrubel, Th., & Kunze, H.-J. 1996, J. Phys. B, 29, 4107
Calisti, A., Khelfaoui, F., Stamm, R., & Talin B. 1990, Phys. Rev. A, 42, 5433
Davies, J. T., & Vaughan, J. M. 1963, ApJ. 4, 1302
Eberhagen, A., & Wunderlich, R. 1970, Z. Physik 232, 1
Einfeld, D., & Sauerbrey, G. 1976, Z. Naturforsch., 31a, 310
Gawron, A., Maurmann, S., Böttcher F., et al. 1988, Phys. Rev. A, 38, 4737
Gigosos, M. A., Mar, S., Pérez, C., & de la Rosa I. 1994, Phys. Rev. E, 49, 1575
Glenzer, S., Uzelac, N. I., & Kunze H.-J. 1992, Phys. Rev. A, 45, 8795
Glenzer, S., Wrubel, Th., Büscher S., et al. 1994, J. Phys. B, 27, 5507
Godbert, L., Calisti, A., Stamm, R., et al. 1994, Phys. Rev. E, 49, 5889
González, V. R. 1999, Ph.D. Thesis, Univ. Valladolid

González, V. R., Aparicio, J. A., del Val, J. A., & Mar S. 2000, A&A, 363, 1177
Greene, R. L. 1976, Phys. Rev. A, 14, 1447
Griem, H. R., Kolb, A. C., & Shen K. Y. 1962, U.S. Naval. Res. Lab. Rept. 5805
Hammel, B. A., Keane, C. J., Cable, M. D., et al. 1993, Phys. Rev. Lett., 70, 1263
Jenkins, J. E., & Burgess, D. D. 1971, J. Phys. B, 4, 1353
Jones, L. A., Greig, J. R., Oda, T., & Griem, H. R. 1971, Phys. Rev. A, 4, 833
Kepple, P. C. 1972, Phys. Rev. A, 6, 1
Konjević, N., Stefanović, I., & Ivković, M. 1995, in Proc. 12th Int. Conf. on Spectral Line Shapes (Toronto, 1994), ed. J. R. Drumond, A. D. May, & E. Oks (New York), 58
Kunasz, P. B. 1980, ApJ, 237, 819
Mar, S., Pérez, C., González, V. R., et al. 2000, A&AS, 144, 509
van der Mullen, J. A. M. 1990, Phys. Rep. 191, 109
Oda, T., & Kiriyama, S. 1980, J. Phys. Soc. Jpn 49, 385
Pérez, C., de la Rosa, M. I., de Frutos, A. M., & Mar S. 1991, Phys. Rev. E, 44, 6785
Piel, A., & Slupek, J. 1984, Z. Naturforsch. 39a, 1041
Pittman, T. L., Voigt P., & Kelleher, D. E. 1980, Phys. Rev. Lett., 45, 723
Pittman, T. L., & Fleurier, C., 1986, Phys. Rev. A, 33, 1291
Rodríguez, F., Aparicio, J. A., de Castro, A., et al. 2001, A&A, 372, 338
de la Rosa, M. I., Pérez C., de Frutos, A. M., & Mar S. 1990, Phys. Rev. A, 42, 7389
Schöning, T., & Butler, K. 1989, A&A, 219, 326
Schöning, T., & Butler, K. 1989, A&AS, 78, 51
Seaton, M. J. 1990, J. Phys. B, 23, 3255
Shrader, C. R., Singh, K. P., & Barrett P. 1997, ApJ, 486, 1006
Soltwisch, H., & Kusch, H. J. 1979, Z. Naturforsch., 34a, 300
Stehlé, C. 1994, A&A, 292, 699
Stehlé, C. 1996, Phys. Scr. T65, 183
Stefanović, I., Ivković, M., & Konjević, N. 1995, Phys. Scr., 52, 178
del Val, J. A., Mar, S., Gigosos, M. A., et al. 1998, Jap. J. Appl. Phys., 37, 4177
del Val, J. A., Aparicio, J. A., González, V. R., & Mar, S. 2000, A&A, 357, 1137
del Val, J. A., Aparicio, J. A., González, V. R., & Mar, S. 2001, J. Phys. B, 34, 2513
Tylenda, R., Stasinska, G., Acker, A., & Stenholm, B. 1994, A&AS, 106. 559
Wrubel, Th., Glenzer, S., Büscher, S., & Kunze, H.-J. 1997, in Proc. 13th Int. Conf. on Spectral Line Shapes (Firenze, 1996), ed. M. Zoppi, & L. Ulivi (New York), 71